Spectral Analysis by the Method of Consistent Constraints

Nikolay V. Prokof'ev[1,2] and Boris V. Svistunov[1,2]

[1] *Department of Physics, University of Massachusetts, Amherst, MA 01003, USA*
[2] *Russian Research Center "Kurchatov Institute", 123182 Moscow, Russia*

(Dated: April 19, 2013)

Two major challenges of numeric analytic continuation—restoring the spectral density, $s(\omega)$, from corresponding Matsubara correlator, $g(\tau)$—are (i) producing the most smooth/featureless answer for $s(\omega)$, without compromising the error bars on $g(\tau)$, and (ii) quantifying possible deviations of the produced result from the actual answer. We introduce the method of consistent constraints that solves both problems.

arXiv:1304.5198v1 [cond-mat.stat-mech] 18 Apr 2013

A dynamic linear-response function can be obtained from the associated Matsubara correlator by analytic continuation of the latter. A prototypical example is the ground-state single-particle Matsubara Green's function in imaginary-time representation, $g(\tau)$. If $g(\tau)$ is specified numerically [1], the procedure of analytic continuation—often referred to as spectral analysis—amounts to finding an appropriate spectral function $s(\omega)$ related to $g(\tau)$ by an integral equation. In our prototypical case, the equation reads (here the function $s(\omega)$ is known to be identically zero at $\omega < 0$ and non-negative at $\omega \geq 0$)

$$g(\tau) = \int_0^\infty \mathrm{e}^{-\omega\tau} s(\omega)\, d\omega\,. \qquad (1)$$

The notorious difficulty of the problem comes from the fact that finding $s(\omega)$ does not reduce to the requirement that the integral in the right-hand side of (1) reproduces the values of $g(\tau)$ within their error bars. Being ill posed, i.e. subject to the sawtooth instability, the problem of numerically finding $s(\omega)$ features infinitely many solutions, ranging continuously from very smooth to extremely noisy ones. It is crucial, thus, not only to satisfy Eq. (1) for a specified set of τ-points, but also to guarantee that $s(\omega)$ is free of sawtooth artifacts. The following two approaches work rather well in achieving this goal: (i) the stochastic-optimization method (SOM) [2] and (ii) the maximum entropy method (MEM) [3, 4]. Within SOM, one employs a stochastic process of minimizing the standard χ^2-measure to produces a large number of noisy solutions, and then takes an average of all the solutions, which is a legitimate procedure thanks to linearity of Eq. (1). In the statistical limit, the outcome of SOM is a rather smooth function as the sawtooth artifacts are averaged out. By construction, the accuracy of reproducing $g(\tau)$ with $s(\omega)$ is not compromised, but, speaking generally, with SOM one cannot guarantee that the final result for $s(\omega)$ is the smoothest of all the functions consistent within the error bars of $g(\tau)$. MEM is complimentary to SOM in the sense that, on one hand, it does guarantee that the outcome for $s(\omega)$ is the best one within a certain class of smooth functions (this class is selected by formulating a "target" or "default" model for the solution, see [3, 4]). On the other hand, smooth solutions are produced at the expense of a systematic bias introduced by the default model; the bias becomes more pronounced as the error bars on $g(\tau)$ are decreased.

Existing methods of spectral analysis, with MEM and SOM as characteristic examples, seem to follow the general principle (cf., e.g., Tikhonov-Phillips regularization methods [5–7]) that there is always a compromise between the requirement of $s(\omega)$ being as smooth as possible and the requirement of reproducing $g(\tau)$ within the error bars.

In this Letter, we show that the "compromise principle" is a mere prejudice. It is possible, and relatively easy (!), to meet the condition of smoothest possible $s(\omega)$ while perfectly respecting the error bars on $g(\tau)$. The price that one has to pay for this luxury is the necessity to introduce a feedback loop locally adjusting the smoothness constraints on $s(\omega)$ to ensure consistency with the error bars on $g(\tau)$. More importantly, the method of consistent constraints (MCC) has a simple built-in tool of quantifying the accuracy of $s(\omega)$.

The issue of quantifying the accuracy of $s(\omega)$ is yet another challenge for the problem of spectral analysis. The sawtooth instability implies that any error bar on $s(\omega)$ should necessarily be of a *conditional* character. The condition which we adopt (finding it natural) is as follows. Any function $s(\omega)$ that we include into the class of legitimate deviations from the optimal (i.e. most smooth) solution is subject to the constraint of not having extra qualitative features like, e.g., extra bumps or minima (more specifically, the constraint is to keep the same structure of sign-domains of the second derivative, see below). With this constraint—clearly justified in the asymptotic regime of appropriately small error bars on the function $g(\tau)$—we employ MCC to deliberately distort the function $s(\omega)$ at a certain $\omega = \omega_*$ and see the extent to which the distortion remains consistent with the error bars of $g(\tau)$.

Illustrative examples. Leaving technical description of the MCC numeric protocol to the second half of the paper, here we consider two illustrative examples. Figures 1 and 2 show the results (cases A and B, respectively) of applying MCC to determine spectral functions for $g(\tau)$ specified numerically with known error bars. Corresponding functions $s(\omega)$ are shown along with their exact

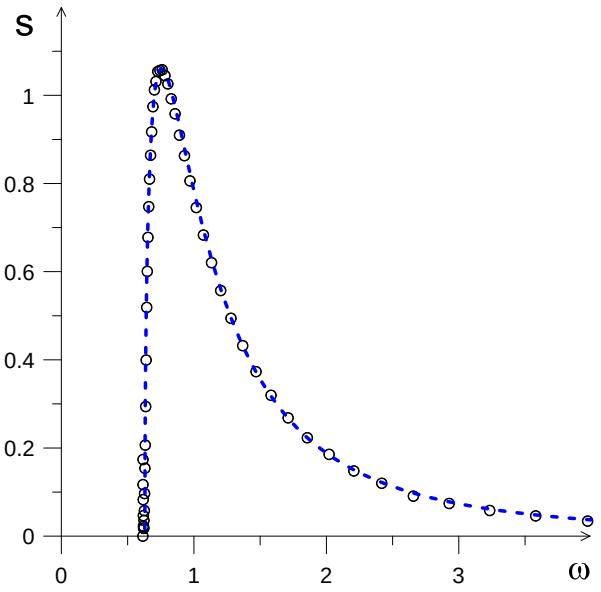

FIG. 1. Case A: The function $s(\omega)$ (circles), obtained by spectral analysis, is very close to the exact spectral density $s_e(\omega)$ (dashed line). The task for the error analysis is to confirm small error bars on $s(\omega)$ without knowing $s_e(\omega)$.

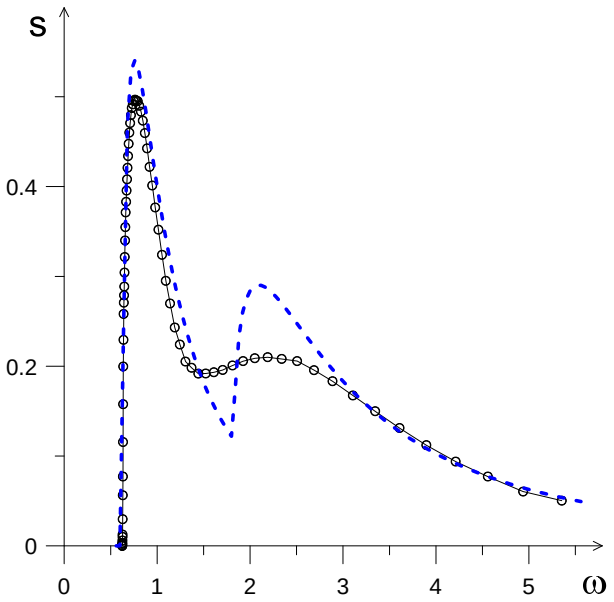

FIG. 2. Case B: Close to the second peak, the function $s(\omega)$ (circles), obtained by spectral analysis, is substantially smother than its exact counterpart $s_e(\omega)$ (dashed line). The challenge for the error analysis here is to characterize possible deviations of $s(\omega)$ from $s_e(\omega)$, without knowing the latter.

counterparts $s_e(\omega)$. The functions

$$g_s(\tau) \;=\; \int_0^\infty \mathrm{e}^{-\omega\tau} s(\omega)\, d\omega \tag{2}$$

coincide with $g(\tau)$ within the error bars on the latter, while the functions $s(\omega)$ are quite smooth. Now we have to characterize possible deviations of $s(\omega)$ from $s_e(\omega)$—pretending that the latter is unknown—making sure that what we get is consistent with the deviations we see in the two figures. In Fig. 3 we show how we quantify the uncertainty of the sharpness of the second peak. The error bars for both cases are presented in Figs. 4 and 5. The asymmetry of the error bars reflects the tendency of the reference solution to broaden sharp features. Apart from the error bar asymmetry, *correlations* between the errors are very informative, as is clear from Fig. 3.

Objective function. Numerically, the left hand side of Eq. (1) is known on a discrete set of τ-points $\tau = (\tau_1, \tau_2, \ldots, \tau_N)$ and $g(\tau_i)$ values have statistical error bars σ_i. The solution for the spectral function will be defined on a dense enough set of frequency points $\omega = (\omega_1, \omega_2, \ldots, \omega_N)$ so that the integral in Eq. (1) is transformed into the finite-sum expression defining a set of $g_s(\tau_i)$ values

$$g_s(\tau_i) = \sum_{j=1}^{M} s_j\, e^{-\omega_j \tau_i}\ . \tag{3}$$

The objective function to be minimized in the process of searching for the smooth solution $s(\omega_j)$ involves several terms $O = \sum_k O_k$. In what follows we describe the minimal number of objectives which allow one to achieve the final goal (all results presented in this Letter were based on them). The first and most important term is the standard χ^2 measure which penalizes differences $g(\tau_i) - g_s(\tau_i)$ outside of the computed error bars, σ_i. For simplicity, we write this measure for the case of uncorrelated statistical errors

$$O_1 = N\chi^2 = \sum_{i=1}^{N} \left[\frac{g(\tau_i) - g_s(\tau_i)}{\sigma_i}\right]^2 . \tag{4}$$

The major goal is to have this objective of the order of unity. Penalty for first derivatives is preventing the development of the saw-instability, i.e. fast changing solutions are disfavored

$$O_2 = \sum_{j=1}^{M-1} D_j^2\, d_j^2\ . \tag{5}$$

To simplify notations, we introduced $d_j = |s_{j+1} - s_j|$. Since the minimization of quadratic form does not guarantee that the solution is non-negative, we also need a penalty which suppresses the amplitudes of the solution

$$O_3 = \sum_{j=1}^{M} A_j^2\, s_j^2\ . \tag{6}$$

Finally, we introduce penalty for the solution to deviate from some "target" form $\bar{s}_j$ for $j = (2, \ldots, M-1)$:

$$O_4 = \sum_{j=2}^{M-1} T_j^2\, (s_j - \bar{s}_j)^2\ . \tag{7}$$

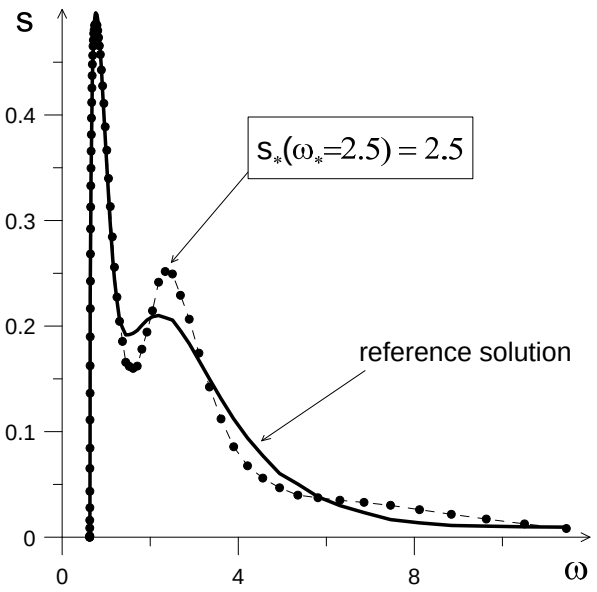

FIG. 3. Example of error analysis for the case B. Shown with a solid line is the reference (the smoothest) solution $s(\omega)$, previously presented in Fig. 2. The solution $s_*(\omega)$ is obtained by pulling the solution up—without compromising the deviation of $g_s(\tau)$ from $s(\omega)$—at the point $\omega = 2.5$ corresponding to the maximum of the second peak. The solution $s_*(\omega)$ corresponds to the threshold of appearance of an extraneous feature, a shoulder at $\omega \approx 6.5$ (that will develop into a bump if we keep pulling up). In this sense, $s_*(\omega)$ characterizes maximal potential deviation of the reference solution from the exact one in the vicinity of the second peak, cf. Fig. 2.

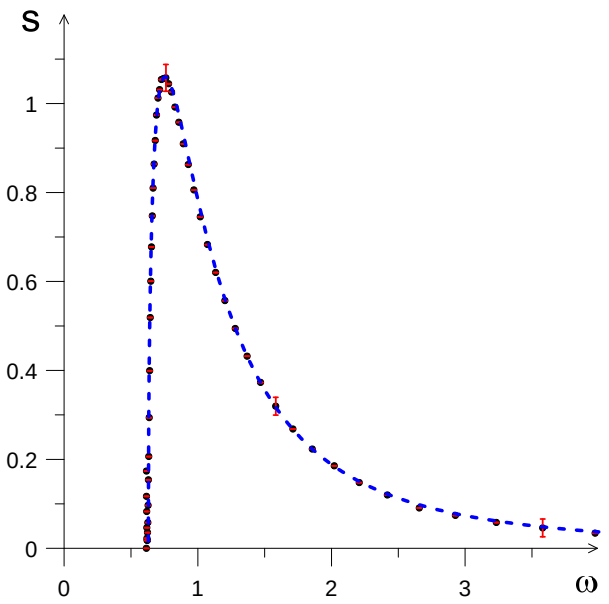

FIG. 4. Case A with three characteristic error bars (cf. Fig. 1).

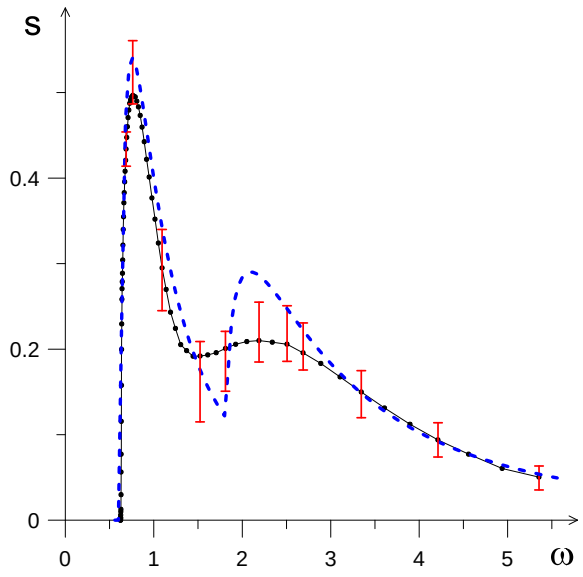

FIG. 5. Case B with the error bars (cf. Figs. 2 and 3). The error bars are essentially asymmetric, reflecting the tendency of the reference solution to broaden sharp features.

There is nothing new in the idea of introducing regularization measures similar to O_2, or Q_4 [3, 5–7] but in the past it was done with j-independent coefficients considered essentially as input parameters (ultimately optimized to achieve the best, but somewhat compromised, χ^2). In our scheme, it is absolutely crucial that constraints control every point of the solution and are adjusted by the feedback loop to be consistent with the properties of the solution itself. Only in this case do we have a guarantee that in the limit of vanishingly small error bars on $g(\tau)$ the final solution will always reach the $\chi^2 \sim 1$ limit.

MCC protocol. Given an objective based on the positive definite quadratic form for s_j, one can relatively easily find the solution minimizing it, $s_j^{(\mathrm{opt})}(O)$, e.g. by the gradient method. This solution, however, may have two serious drawbacks: It may contain negative values of s_j and be far from meeting the crucial requirement of having $\chi^2 \sim 1$. The following self-consistent iterative protocol is designed to eliminate both shortcomings.

1. Let index k denote the number of performed iterations. Start with $k = 0$, some initial solution $s_j^{(0)}$, large penalties for first derivatives $D_j^{(0)}$, and zero values of $A_j^{(0)}$. Define $\bar{s_j}^{(0)} = (s_{j+1}^{(0)} + s_{j-1}^{(0)})/2$ for $j = 2, \ldots, M-1$.

We find it sufficient to have $T_j^{(k)} = D_j^{(k)}$ for any k (with small modification in the protocol quantifying error bars, see below), but one is free to design other rules for these coefficients.

2. Determine the next iteration solution by minimizing the objective function, $s_j^{(k+1)} = s_j^{(\mathrm{opt})}(O^{(k)})$; set $k \to k+1$.

3. Since Q_1 term is the only reason for having a non-flat result, the solution is now analyzed to adjust the objective so that penalties compromising the χ^2 measure are reduced, and penalties for developing the negative solution are increased: If $d_j^{(k)}$ exceeds $C/D_j^{(k-1)}$ (in practice, we use $C = 0.1$) then

$$D_j^{(k)} = C/d_j^{(k)} \ . \tag{8}$$

Otherwise, the penalty is considered to be too conservative and is increased as $D_j^{(k)} = 2D_j^{(k)}$. To prevent divergent behavior, determine $D_{\min} = min\{D_j\}$ and restrict allowed values to $rD_{\min}$, where r is some large number (typically of order of 10^3). After that set $T_j^{(k)} = D_j^{(k)}$.

4. If $s_j^{(k)} < 0$ introduce large penalty $A_j^{(k)} = A_{\max}$ (it can be as large as 10^8) to prevent the solution from going negative in the next iteration. If $s_j^{(k)} > 0$ decrease the penalty, $A_j^{(k)} = A_j^{(k-1)}/10$ (for positive values of the solution A-coefficients decay exponentially fast with the number of iterations).

5. Finally, set $\bar{s_j}^{(k)} = (s_{j+1}^{(k)} + s_{j-1}^{(k)})/2$ to stabilize second derivatives of the solution. This determines the new objective function $O^{(k)}$. Proceed to step 2.

In essence, the procedure adjusts regularization parameters by feedback from the solution itself and ultimately has them small enough to admit a solution of Eq.(1) within the error bars, and large enough to have a smooth solution. If there are δ-functional peaks in the spectral function one should add them to the solution at some locations and exclude their amplitudes from the objectives O_2 and O_4 for obvious reasons. The nature and stability of the MCC feedback loop is also compatible with interrupting it from time to time and suggesting modifications to the existing solution which minimize only the χ^2—the subsequent MCC protocol quickly erases unwanted ripples. We also find it useful to "level-off" large point-to-point fluctuations in the regularization parameters after several feedback loops.

The protocol of examining error bars on s_j is identical to the one described above except that for some frequency point $\omega_m = \omega_*$ the target parameter $\bar{s}_m$ remains fixed at some predetermined value s_* and T_m is made large enough to suppress significant deviations of the solution from s_*. As we increase/decrease the value of s_* we ultimately observe that either the value of χ^2 is increased by a factor of two, or a new feature appears on the curve. This determines the error margins on the final solution. [Since in the protocol of determining error bars on s_j the values of $\bar{s}_m$ and T_m are excluded from the feedback loop the χ^2 measure may increase as we "pull" the point due to hysteresis effect.]

Discussion. As is seen from the above-described protocol, the central idea of MCC is to iteratively adjust—tighten/relax—regularization constraints, by feedback from the solution $s(\omega)$ that minimizes the objective function for the previous iteration. The choice of constraints is rather wide; they can deal with the values of the function $s(\omega)$, as well as with the values of its first and higher derivatives; within one and the same iteration, or addressing previous iterations as well. The crucial common feature is the locality of constraints in ω-space, which readily allows one to judge—see steps 3 and 4 of the protocol—whether constraints are (i) too restrictive, (ii) too loose, or (iii) perfectly consistent. Performancewise, it is due to those simple *local* measures of consistency of each specific constraint that feedback iterations rapidly fine-tune the objective function to be the most restrictive—while remaining free of systematic bias—within the error bars of the function $g(\tau)$.

In principle, the set of consistent constraints can be extended to include any knowledge about likely features of the function $s(\omega)$. For example, expecting a simple monotonic asymptotic behavior in the tail, one may opt to severely penalize wrong signs of (higher) derivatives, similarly to penalizing negative values of $s(\omega)$.

The MCC protocol can be applied to any problem of restoring a function from a representative set of its integrals with an arbitrary kernel. An immediate example is the numeric function $g(\tau)$ itself, when it comes from a Monte Carlo simulation in terms of integrals of $g(\tau)$ over a number of intervals ("bins"). An accurate value of $g(\tau)$ for any τ can then be extracted by the MCC—either directly, or as a by-product of restoring $s(\omega)$ from the bin integrals.

In absorption spectroscopy, MCC can be used for unbiased restoring unknown density distribution from binned absorption images, or just to produce a smooth—still unbiased (!)—image from data integrated over bins.

This work was supported by the National Science Foundation under grant PHY-1005543, and by a grant from the Army Research Office with funding from DARPA.

[1] The majority of first-principle numeric approaches to equilibrium statistics of quantum many-body systems deal with imaginary-time Matsubara correlation functions.
[2] A.S. Mishchenko, N.V. Prokof'ev, A. Sakamoto, and B.V. Svistunov, Phys. Rev. **B 62**, 6317 (2000).
[3] R.N. Silver, D.S. Sivia, and J.E. Gubernatis, Phys. Rev. **B 41**, 2380 (1990).
[4] M. Jarrell and J.E. Gubernatis, Phys. Rep, **269**, 133 (1996).
[5] A.N. Tikhonoff, Doklady Akademii Nauk USSR **151**, 501 (1963) [Soviet Mathematics **4**, 1035 (1963)].
[6] D.L. Phillips, J. ACM **9**, 84 (1962).
[7] R. Blankenbecler, D.J. Scalapino, and R.L. Sugar, Phys. Rev. **D 24**, 2278 (1981).